

# High efficiency n-type PERT and PERL solar cells

Jan Benick, Bernd Steinhauser, Ralph Müller, Jonas Bartsch, Mathias Kamp, Andrew Mondon, Armin Richter, Martin Hermle, Stefan Glunz

Fraunhofer Institute for Solar Energy Systems, Freiburg, Baden Wuerttemberg, 79110, Germany

**Abstract** — *n*-type PERT and PERL structures both offer a high efficiency potential. In this work we applied ion implantation for the realization of both the emitter and the BSF of high-efficiency PERT and PERL structures and laser processes for local BSF formation showing efficiency benchmarks for those in principle industrially feasible technologies. For a fully ion implanted PERT solar cell we reached efficiencies up to 22.7%, showing that even at this high level no residual implantation damage is left and the  $V_{oc}$  is limited by the profiles themselves. For the PERL structure we applied the PassDop process using two different passivation layer systems (based on  $SiC_x$  and  $SiN_x$ ). With this laser based process we were able to reach conversion efficiencies up to 23.2%, showing that the laser doping process is as efficient as a PERL rear side realized by photolithography. To prove the industrial feasibility of these high-efficiency solar cell concepts we applied Ni plating as front side emitter metallization on a PassDop solar cell featuring a boron implanted emitter. For this cell type we were able to reach an efficiency of 21.7% in a first prove of principle batch.

**Index Terms** — *n*-type, high-efficiency, implantation, laser

## I. INTRODUCTION

*n*-type PERT and PERL solar cells structures both offer a high efficiency potential. However, industrially feasible ways for the fabrication of these high efficiency devices are needed. For the doping of the emitter as well as the full area and the local BSF processes need to be developed which allow for an easy single side processing as well as a reproducible, damage free and high quality fabrication of the doped areas.

For the front side boron emitter as well as the full area BSF of a PERT solar cell, ion implantation has been identified as a promising technology, as the process itself is truly single sided and no doped glass is needed [1-3]. For the formation of the local BSF we developed a laser based process using a doped passivation layer [4].

To achieve highest efficiencies, metallization technologies beyond screen printing are needed. Using plated contacts, many of the so far existing challenges for metallizing high-efficiency *n*-type devices can be overcome. As plated contacts have many similarities with evaporated contacts, the efficiency potential of this technology is quite high and industrial implementation is possible.

In this paper the recent developments in the field of high-efficiency *n*-type solar cells will be given, with the main focus on ion implantation, the PassDop process as well the combination of ion implantation, PassDop and a front side metallization based on plating.

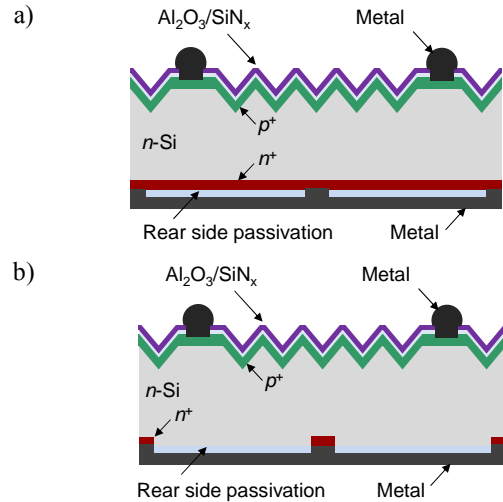


**Figure 1** Schematic drawing of two high-efficiency *n*-type solar cell structures: a) PERT solar cell, b) PERL solar cell.

## II. ION IMPLANTATION

Ion implantation is known for very precise control and reproducibility of impurity doping and thus has been established as the standard doping process in CMOS fabrication. In photovoltaics ion implantation is an interesting alternative for tube furnace diffusion processes. Ion implantation inherently is a single side process which can be easily masked by shadow masks. No doped glass (PSG, BSG) is formed during the doping process. Especially for the realization of boron doped areas, where the diffusion process is known to be more complicated than for phosphorus, ion implantation might be a promising option. In several publications it has been shown, that the damage introduced during implantation can be removed by an annealing step, leading to emitter saturation current densities below  $10 \text{ fA/cm}^2$  on both phosphorus and boron doped areas respectively [5].

For the doping profiles applied for the PERT solar cells (see Figure 2) the intrinsic  $J_{0e}$ , i.e. the  $J_{0e}$  which is caused by intrinsic losses within the profile, has been calculated with EDNA [6]. The calculated  $J_{0e}$ , taking into account the respective surface recombination velocity taken from diffused references, shows a perfect match with the measured data.

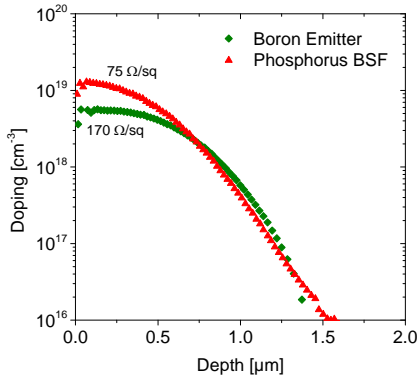


**Figure 2** Doping profiles of the fully implanted PERT solar cell.

**Table I:** Fully implanted PERT solar cell (2x2 cm<sup>2</sup>).

Cell type	$V_{oc}$ mV	$J_{sc}$ mA/cm <sup>2</sup>	$FF$ %	$pFF$ %	$\eta$ %
PERT	691	40.9	80.2	83.8	22.7*

\* Certified by Fraunhofer ISE CalLab

Fully implanted PERT solar cells featuring the doping profiles shown in Figure 2 have been fabricated. The basic structure of the cells is shown in Figure 1a. After front side texturing the cells received the implantation processes for emitter and BSF. For the annealing of the implanted profiles a common high temperature step has been used. The oxide grown during this step also has been used as the rear side passivation. The front side boron emitter was passivated by a stack consisting of a thin Al<sub>2</sub>O<sub>3</sub> (10 nm, PA-ALD), SiN<sub>x</sub> (50 nm, PECVD) and MgF<sub>2</sub> (100 nm, evaporation) to form a double layer antireflection coating (DARC). The contact openings were formed with photolithography and the front and rear side metal was evaporated (front: Ti/Pd/Ag, rear:Al). The front side contacts were thickened by an Ag plating step.

With these laboratory scale fully implanted high-efficiency PERT solar cells we were able to achieve a conversion efficiency of 22.7% (see Table I). The cells show a very high  $V_{oc}$  of 691 mV, limited mainly by rear side recombination due to the BSF doping profile. For the applied doping profiles the  $V_{oc}$  level of 691 mV achieved for the PERT solar cell is close to the theoretical limit of 695 mV that can be obtained with the applied doping profiles (see Table II). For a uniformly doped BSF there is always a compromise between contacting and recombination at the metal contacts and the passivated regions, i.e. a certain surface concentration is required to allow for an efficient ohmic rear side contact.

**Table II:** Saturation current density of the respective parts of the fully implanted PERT solar cell. The metalized fraction is 1.1 % for the front side and 0.7% for the rear side (point contacts with a diameter 20 μm of and a pitch of 250 μm).

	Emitter	BSF	Metal front	Metal rear	Bulk	Total
$J_{0e}$ [fA/cm <sup>2</sup> ]	12	29	16	4	10	71

The high quality of the fully ion implanted PERT solar cell is also confirmed in the high quantum efficiency shown in Figure 3.

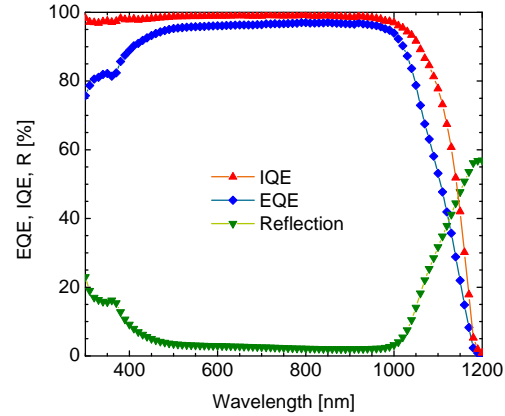


**Figure 3** EQE and IQE of the fully implanted PERT solar cell.

### III. PASSDOP

In order to achieve high conversion efficiencies a passivated rear side has to be applied. The rear side structure featuring the highest efficiency potential is the PERL structure with only a local BSF underneath the rear side contact points. With the “PassDop” concept shown in Figure 4, an elegant way for the realization of such a structure has been shown [4].

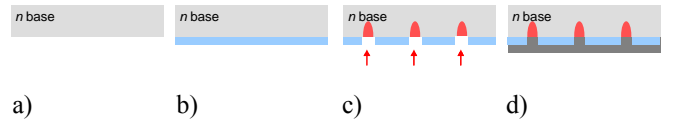


**Figure 4** Schematic of the PassDop process. On top of the bare rear side (a) a phosphorus doped dielectric layer is deposited (b). In a subsequent laser process the dielectric layer is locally opened (c) and the dopant is driven into the silicon. In a last step a metal layer is deposited (d).

For the dielectric passivation we apply two different approaches, i) a-SiC<sub>x</sub>:P based layer system and ii) a-SiN<sub>x</sub>:P based layer system. The properties of the resulting doping profiles for the local BSF after the laser process are given in Table III. As can be seen, with both layers appropriate BSF doping with sheet resistances  $\leq 30 \Omega/\text{sq}$  and a surface concentration  $> 3 \times 10^{19} \text{cm}^{-3}$  can be reached.

**Table III:** Properties of the local BSF for the a-SiC<sub>x</sub> and a-SiN<sub>x</sub> based PassDop layers respectively

	$R_{\text{sheet}}$ [ $\Omega/\text{sq}$ ]	$N_{\text{surface}}$ [ $\text{cm}^{-3}$ ]	Depth [ $\mu\text{m}$ ]
a-SiC <sub>x</sub> :P	~15	~ $8 \times 10^{19}$	~3.5
a-SiN <sub>x</sub> :P	~30	~ $3 \times 10^{19}$	~3

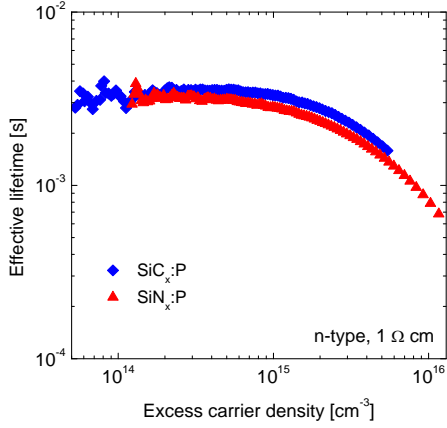


**Figure 5** Measured effective lifetimes for the SiC<sub>x</sub> and SiN<sub>x</sub> based PassDop layers, respectively.

Both layers exhibit excellent surface passivation properties. As can be seen in Figure 5 effective lifetimes in the range of 3 ms can be reached on 1  $\Omega$  cm *n*-type silicon for both layers ( $S_{\text{eff}} < 5 \text{ cm/s}$ ), making them perfectly suited for the application as the rear side passivation of a PERL type solar cell.

Both layers have been applied at the device level, i.e. high-efficiency laboratory type solar cells (area: 4 cm<sup>2</sup>). The basic structure of the cells is shown in Figure 1b. After texturing and boron emitter diffusion on the front side the solar cell surfaces are passivated. A stack consisting of a thin Al<sub>2</sub>O<sub>3</sub> (10 nm, PA-ALD) and SiN<sub>x</sub> (60 nm, PECVD) is applied for the front side emitter, the rear side is passivated by the *PassDop* stack based either on the a-SiC<sub>x</sub>:P or the a-SiN<sub>x</sub>:P (PECVD). After surface passivation the front side contacts were realized by photolithography and evaporating a seed layer of Ti/Pd/Ag. In the next step the rear side contact opening as well as the local doping was realized by a laser process before the rear side contacts were formed by evaporation of Al. As a last step the front side contacts were thickened by plating of Ag.

The results of the I-V measurements are summarized in Table IV. As can be seen, with both approaches very high conversion efficiencies up to 23.2% for the SiC<sub>x</sub> and 22.8% for the SiN<sub>x</sub> based PassDop were reached so far.

The high  $V_{\text{oc}}$  level that has been reached for both approaches proves the excellent rear side passivation of the applied dielectric layers based on SiC<sub>x</sub> and SiN<sub>x</sub> respectively. The

high fill factors >80.5% also show that a good contact can be formed to the local doping at the rear side.

**Table IV:** PERL solar cell with different rear side PassDop layers.

	Material	$V_{\text{oc}}$ [mV]	$J_{\text{sc}}$ [mA/cm <sup>2</sup> ]	$FF$ [%]	$pFF$ [%]	$\eta$ [%]
SiC <sub>x</sub> :P	Cz, 1.7 $\Omega\text{cm}$	699	41.3	80.5	84.0	23.2*
SiN <sub>x</sub> :P	FZ, 0.5 $\Omega\text{cm}$	693	40.6	80.8	83.5	22.8*

\* Certified by Fraunhofer ISE CalLab

The high quality of the fully ion implanted PERT solar cell is also confirmed in the high quantum efficiency shown in Figure 6

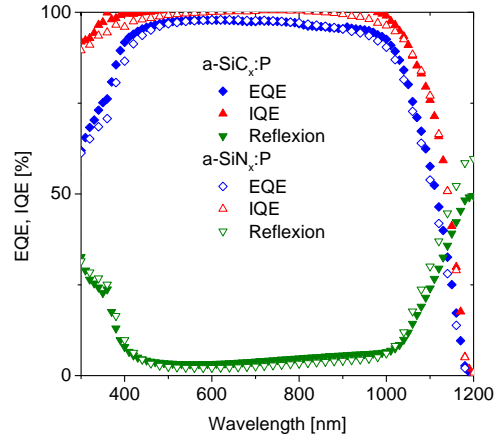


**Figure 6** EQE and IQE of the a-SiC<sub>x</sub>:P and the a-SiN<sub>x</sub>:P based *PassDop* solar cell.

Therefore the *PassDop* technology is a quite promising approach for the fabrication of high-efficiency *n*-type solar cells.

#### IV. PLATING

Low resistivity contacts on boron emitters are hard to achieve by standard printing, especially for low boron surface doping concentrations as applied for the cells show in the previous sections. Also a voltage reduction of ~30 mV by currently available printing paste generation has been reported [7,8]. Consequently, the metal-semiconductor contact for the highest efficiencies on boron emitters might be based on plating.

Plated nickel as contacting material has been shown to allow comparable performance to evaporated Ti/Pd/Ag on lowly doped phosphorous and boron emitters [9,10]. It can be reinforced by plated copper and tin to form a silver-free, highly conductive and industrially feasible contact system.

In principle, this contact system is quite similar to the high efficiency laboratory approach. In both cases, the formation of a silicide is realized to adjust contact properties by contact formation at relatively low temperatures (250-450°C), allowing for temperature sensitive passivation layers.

The Ni/Cu/Sn plating process has been applied to SiN<sub>x</sub>:P based *PassDop* solar cells featuring a boron implanted emitter with a profile slightly higher doped ( $R_{\text{sheet}} \sim 90 \Omega/\text{sq}$ ) as the one shown in Figure 2. The 15  $\mu\text{m}$  front contact opening was realized using photolithography and wet etching. The rear side of the cells was metallized by evaporated aluminium. The I-V parameters of the best cell are shown in Table V.

**Table V:** PassDop solar cell with boron implanted emitter and plated Ni/Cu front contacts (2x2 cm<sup>2</sup>).

Cell type	$V_{\text{oc}}$ mV	$J_{\text{sc}}$ mA/cm <sup>2</sup>	$FF$ %	$\eta$ %
PassDop	677	39.6	81.2	21.7*

\* Certified by Fraunhofer ISE CalLab

The  $V_{\text{oc}}$  of  $\sim 680$  mV is slightly lower compared to the cells shown in the previous sections which is due to the higher doped boron emitter as well as to the larger contact opening (15  $\mu\text{m}$  compared to 5  $\mu\text{m}$  for the high-efficiency PassDop cells, leading to a total  $J_{\text{oc}} \sim 70 \text{ fA/cm}^2$ ).

Nevertheless, a high FF >81% could be reached allowing a conversion efficiency of 21.7% for the Ni plated PassDop solar cell. As boron emitter, plating and thermal contact formation are not optimized on these cell structure, further improvements are likely.

## V. CONCLUSION AND OUTLOOK

High-efficiency *n*-type PERT and PERL solar cells featuring an ion implanted boron emitter and a phosphorus BSF realized by ion implantation and laser processes respectively, have been presented, showing an efficiency benchmark for the applied technologies. For the fully implanted PERT solar cells conversion efficiencies up to

22.7% could be reached, which is now mainly limited by the profile shape itself. For the laser based *PassDop* process efficiencies up to 23.2% have been shown.

Combining both ion implanted emitter with the PassDop approach at the rear and applying Ni/Cu plated front contacts we were able to realise a silver free, strictly single side processed high efficiency cell with an efficiency of 21.7%.

## REFERENCES

- [1] T. S. Bösche et al., "Fully ion implanted n-type cells – a contender for industrial cells with >20.5% efficiency", *IEEE Journal of Photovoltaics* 4(1), p. 48-51, 2013.
- [2] A. Rohatgi et al., "High throughput ion-implantation for low cost high-efficiency silicon solar cells", *Energy Procedia* 15, p. 10-19, 2013.
- [3] C.E. Dube et al., "High-efficiency selective emitter cells using patterned ion implantation", *Proceedings of the 1<sup>st</sup> SiliconPV*, Freiburg, Germany, *Energy Procedia* 8, 706-711, 2011.
- [4] D. Suwito et al., "Industrially feasible rear passivation and contacting scheme for high-efficiency n-type solar cells yielding a  $V_{\text{oc}}$  of 700 mV", *IEEE Trans. Electron Devices* 57(8), 2032-2036, 2010.
- [5] J. Benick et al., "Fully implanted n-type pert solar cells", *Proceedings of the 27th European Photovoltaic Solar Energy Conference and Exhibition*, Frankfurt, Germany, 2011.
- [6] K.R. McIntosh, P.P. Altermatt, A freeware 1D emitter model for silicon solar cells, *Proceedings of the 35th IEEE photovoltaics specialists conference*, Honolulu, 2010.
- [7] R. Kopecek, "Overview on n-type solar cell architectures, efficiencies and importance for measurement standards", *Proceedings of the 3rd n-PV Workshop*, Chambéry, France, 2013.
- [8] A. Edler et al., "Metallization-induced recombination losses of bifacial silicon solar cells", *Prog. Photovolt: Res. Appl.*, 201), DOI: 10.1002/pip.2479
- [9] J. Bartsch, et al., "Progress with multi-step metallization featuring copper as conducting layer at Fraunhofer ISE", *Proceedings of the 27th European Photovoltaic Solar Energy Conversion Conference and Exhibition*, Frankfurt, Germany, 2012, pp. 604-607
- [10] J. Bartsch et al., "21.8 % efficient n-type solar cells with industrially feasible plated Metallization", *Proceedings of the 4<sup>th</sup> SiliconPV*, 's-Hetzingenbosch, Netherlands, 2014